

# Evolution of structural and magnetic parameters of nickel nanotubes under irradiation of $\text{Fe}^{7+}$ ions

A. Shumskaya<sup>1</sup>, E. Kaniukov<sup>2</sup>, D. Shlimas<sup>3</sup>,  
M. Zdorovets<sup>3,4,5</sup>, A. Kozlovskiy<sup>\*,3,4</sup>

<sup>1</sup>Scientific-Practical Materials Research Center NAS of Belarus, Minsk, Belarus

<sup>2</sup>National University of Science and Technology «MISIS», Moscow, Russia

<sup>3</sup>L.N. Gumilyov Eurasian National University, Nur-Sultan, Kazakhstan

<sup>4</sup>Institute of Nuclear Physics, Almaty, Kazakhstan

<sup>5</sup>Ural Federal University named after the First President of Russia B.N. Yeltsin, Yekaterinburg, Russia

E-mail: kozlovskiy.a@inp.kz

DOI: 10.29317/ejpfm.2020040204

Received: 20.03.2020 - after revision

This work is devoted to investigations of nickel nanotubes behavior under influence of swift heavy ion irradiation. High-energy irradiation initiates damage process inside nanostructures and can cause the appearance of new phases with interesting properties. To understand the basic principles of the evolution of structural and magnetic parameters of nanostructures under the influence of high-energy processes, detailed study of nickel nanotubes irradiated with various fluences of  $\text{Fe}^{7+}$  ions was carried out.

**Keywords:** nanostructures, irradiation, magnetic structure, nanotubes, swift heavy ions.

## Introduction

Ion irradiation is an attractive method that allows both determining the limits of nanostructures applicability under extreme conditions and investigating change their structure occurring during interaction of nanomaterials with swift heavy ions (SHI). High-energy effect can not only worsen the physical properties of materials, but also allows obtaining nanostructures with novel properties [1-3]. Thus, one of

the important problems of the radiation modification is the controlled formation of defects in the crystal structure in order to improve the functional properties of the material, for example, increasing the strength characteristics or enhancing of nanostructures magnetic parameters [4, 5]. The acquired properties directly depends on the degree of radiation damage, which is related to the irradiation conditions (mainly with energy and fluence) and the type of incident ions [6, 7]. Depending on the irradiation energy, the dynamic processes associated with the deformation of the atomic structure of nanomaterials can be activated, as well as the formation of metastable phases that can lead to partial amorphization, structural deformation and implantation. The fluence of irradiation makes it possible to evaluate the nature of the processes of interaction of incident ions with matter, mechanisms of defect formation and phase transformations [8].

Today great attention is paid to experimental investigations of ion irradiation of nanowires and nanotubes (for example [9-12]) with different type of irradiation with both low ( $<1$  MeV/nucleon) [13, 14] and high energies ( $>1$  MeV/nucleon) [15-18]. In listed papers, results of the studying of changes of structure and composition as well as conductivity of irradiated nanostructures are presented. The correlation between structural changes and magnetic properties is not estimated well. To eliminate this gap, in our work, the study of the morphological and structural features of nanostructures under irradiation, on the example of nickel nanotubes which were irradiated with  $\text{Fe}^{7+}$  ions with fluences up to  $5 \times 10^{11} \text{ cm}^{-2}$ , are considered, and the correlation between the structural changes and the magnetic characteristics is established.

## Materials and methods

The technique of template synthesis with electrolyte  $\text{NiSO}_4 \times 6\text{H}_2\text{O}$  (100 g/l),  $\text{H}_3\text{BO}_3$  (45 g/l),  $\text{C}_6\text{H}_8\text{O}_6$  (1.5 g/l) at potential difference of 1.75 V and temperature  $25^\circ\text{C}$  was used [19, 20]. Templates were PET porous films with pore density  $4.0 \times 10^7 \text{ cm}^{-2}$ , thickness 12 microns and diameters  $380 \pm 20 \text{ nm}$ . Irradiation of nanotubes contained in PET templates was carried out at the "DC-60" heavy ion accelerator of Astana branch of the Institute of Nuclear Physics. As bombarding beams were used  $\text{Fe}^{7+}$  ions with energies of 1.5 MeV/nucleon with fluences ranging from  $1 \times 10^9$  to  $5 \times 10^{11} \text{ cm}^{-2}$ .

Initial and irradiated nanotubes was studied by methods of X-ray diffraction structural analysis, scanning electron microscopy described in [21-23].

Magnetic characteristics of samples were studied on universal measuring system (automated vibrating magnetometer) «Liquid Helium Free High Field Measurement System» (Cryogenic LTD) in magnetic fields  $\pm 2 \text{ T}$  at 300 K temperature.

## Results and discussions

Arrays of nickel nanotubes were synthesized in the pores of the PET templates with length  $(11.7 \pm 0.2 \text{ }\mu\text{m})$  and diameters of  $390 \pm 20 \text{ nm}$ . The general view of

the nickel nanotubes array after removal from the polymer template is shown in Figure 1a.

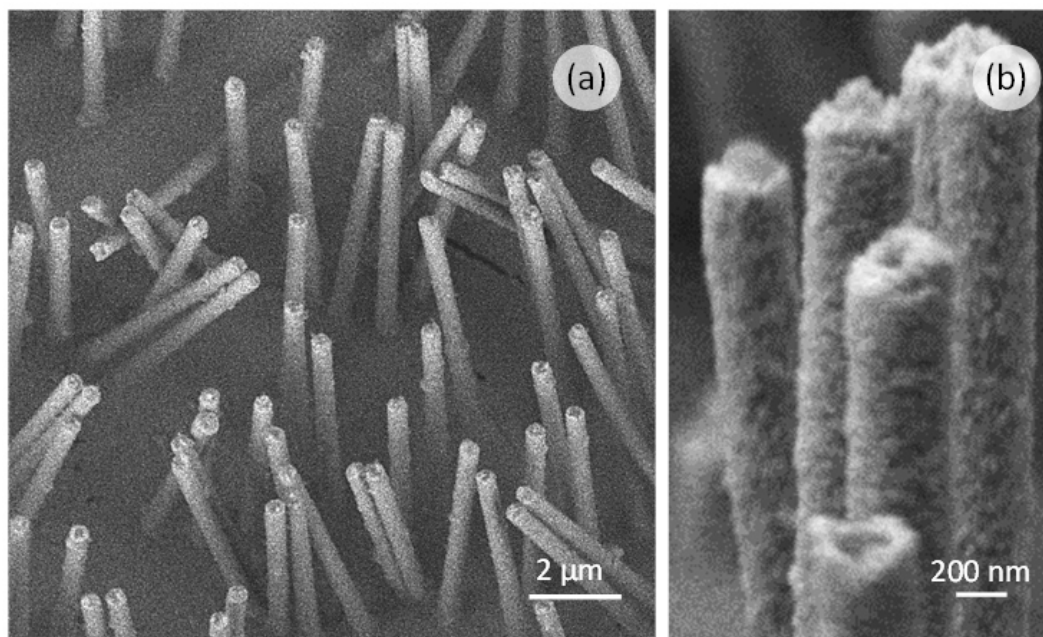


Figure 1. SEM images of pristine nickel nanotubes arrays (a) and enlarged picture (b).

Synthesized arrays of nickel nanotubes in templates were irradiated with different fluence by  $\text{Fe}^{7+}$  ions. Figure 2 shows the dynamics of changes in the morphology of nanostructures as a result of irradiation. As can be seen from the data presented, as a result of an increase in the irradiation fluence, there are no visible structural changes and the formation of cracks and amorphous regions that were observed in the case of light ion irradiation, which indicates the stability of nickel structures to irradiation with  $\text{Fe}^{7+}$  ions. An increase in the irradiation fluence leads to a change in the surface morphology, as well as to the formation of small spherical outgrowths on the surface of the nanotubes which can be caused by the migration of defects to the grain boundaries and, accordingly, to the surface of nanotubes.

Figure 3 shows the data on the changes in X-ray diffraction patterns of the studied samples because of irradiation. According to x-ray phase analysis, the initial samples are polycrystalline Ni structures with a face-centered type of crystal lattice, spatial symmetry Fm-3m (225).

According to XRD analysis, irradiation with  $\text{Fe}^{7+}$  ions leads to the appearance of low-intensity peaks in the diffraction patterns that correspond to the phase of the FeNi interstitial solid solution. The appearance of new FeNi peaks indicates the implantation of  $\text{Fe}^{7+}$  ions in the interstices or lattice sites. In this case, an increase in the irradiation fluence leads to an increase in the peak intensities characteristic of FeNi, which indicates an increase in the content of the impurity phase in the structure.

The increase of the content of the impurity phase may be due to similar chemical properties and ionic radii of Fe and Ni atoms, which leads to the substitution of Fe atoms for Ni atoms in the lattice, followed by the formation of stable compounds of the substitutional solid solution phase. In this case, the appearance of the

interstitial phase leads to distortion and deformation of the structure, as evidenced by an increase in the asymmetric distortion of the diffraction peaks and their shift to the region of small angles. The shift of the diffraction peaks indicates a change in interplanar spacing as a result of the introduction of iron ions into the nodes of the crystal lattice with the subsequent substitution of nickel atoms and the formation of impurity inclusions. The formation of impurity inclusions leads to a sharp decrease in the peak intensity (220), which indicates a reorientation of crystallites as a result of the introduction of  $\text{Fe}^{7+}$  ions. The formation of the interstitial phase, as well as the reorientation of crystallites, is caused by large energy losses of  $\text{Fe}^{7+}$  ions on the nuclei. This leads to the formation of a large number of initially knocked out atoms from the lattice sites, which are replaced by  $\text{Fe}^{7+}$  ions with the subsequent formation of a new phase, which leads to an increase in the crystal structure parameter.

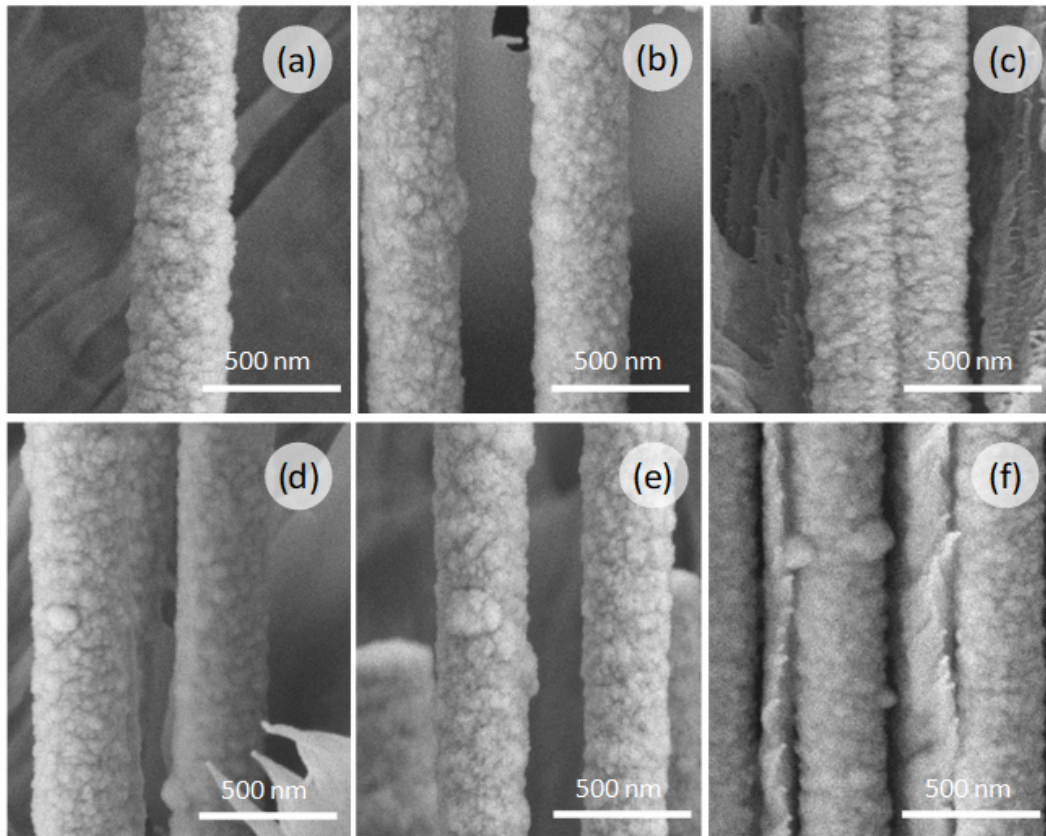


Figure 2. SEM images of Ni nanotubes before and after irradiation with  $\text{Fe}^{7+}$  ions with fluences: (a) initial sample; (b)  $10^9 \text{ cm}^{-2}$ ; (c)  $10^{10} \text{ cm}^{-2}$ ; (d)  $5 \times 10^{10} \text{ cm}^{-2}$ ; (e)  $10^{11} \text{ cm}^{-2}$ ; (f)  $5 \times 10^{11} \text{ cm}^{-2}$ .

Lattice parameter, dislocation density and crystallinity degree were calculated by the methodical, mentioned in [24].

In turn, a change in distortions and deformations in the structure leads to a change not only in structural parameters, but also in the degree of perfection of the crystal structure, as well as a change in the density of dislocation defects (data in Table 1). In this case, an increase in the dislocation density of defects indicates a deformation of the crystal structure and a subsequent increase in the concentration of disordered regions in the crystal lattice.

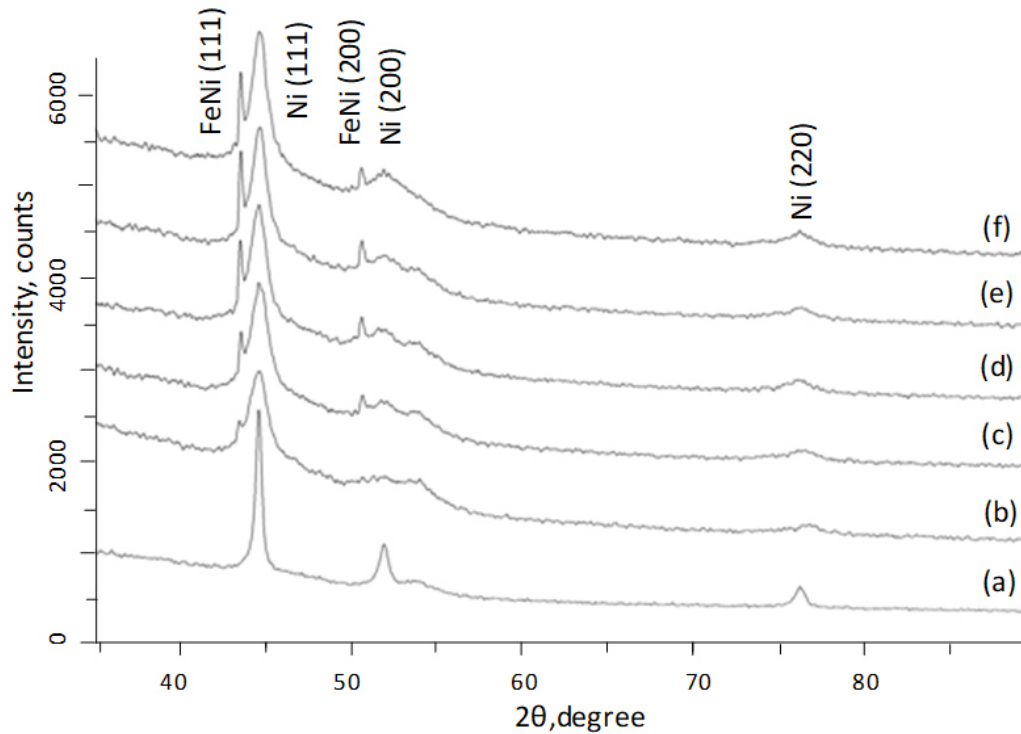


Figure 3. X-ray diffraction patterns of Ni nanotubes arrays before and after irradiation with  $\text{Fe}^{7+}$  ions with fluences.

Table 1.

Dependence of the main structural parameters on the irradiation fluence.

Fluence, $\text{cm}^{-2}$	Lattice parameter, Å	Dislocation density, $\text{m}^{-2} \times 10^{15}$	Crystallinity degree, %
0	$3.4703 \pm 0.0011$	1.56	91
$10^9$	$3.5060 \pm 0.0015$	2.61	89
$10^{10}$	$3.5081 \pm 0.0015$	4.41	87
$5 \times 10^{10}$	$3.5097 \pm 0.0012$	4.55	86
$10^{11}$	$3.5106 \pm 0.0025$	7.06	84
$5 \times 10^{11}$	$3.5298 \pm 0.0022$	7.08	82

To determine the effect of irradiation with Fe ions on main magnetic characteristics of Ni nanotubes, magnetization dependence on the magnetic field  $M(H)$  for parallel and perpendicular field directions respectively to orientation of the nanotubes axis were carried out (Figure 4). Based on hysteresis loops the main magnetic characteristics ( $H_c$  is coercivity,  $M_R/M_S$ , is squareness ratio of hysteresis loop) were determined. These characteristics are presented in Table 2.

The hysteresis loops have a typical form for soft ferromagnetic materials. Some discrepancy in the shape of hysteresis loops for different directions of the magnetic field relatively to the nanotubes axis indicates the presence of magnetic anisotropy. For example, for pristine samples, the coercivity values for a parallel orientation of the field relatively to the nanotube axis ( $H_{C\parallel}$  lies within 50 Oe) are lower than the values for the perpendicular direction of the field ( $H_C = 81$  Oe).

Irradiation of nickel nanotubes with Fe ions leads to a slight change in both the coercivity and the squareness ratio of hysteresis loop (Table 2). Coercivity increases to a value of  $10^{10} \text{ cm}^{-2}$  and decreases after exceeding this fluence for

both directions of the applied field (perpendicular and parallel). The change in squareness ratio of hysteresis loop has a rather unexpected nature.  $M_R/M_S$  for the direction of the magnetic field parallel to the axis of nanotubes decreases, and when the perpendicular field is applied, it increases.

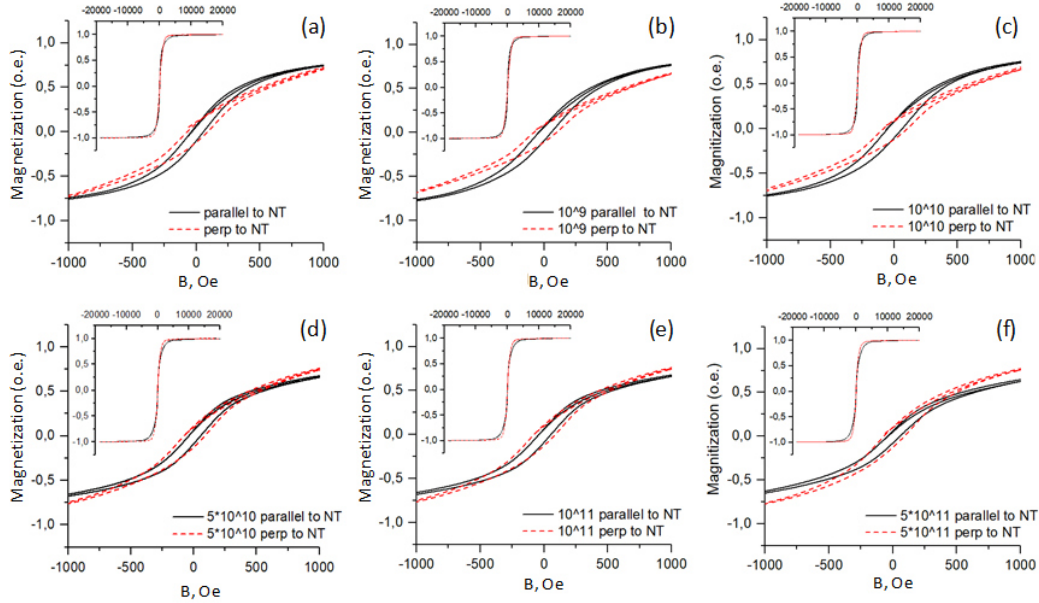


Figure 4. Magnetic characteristics of the samples before and after irradiation for different directions of the magnetic field relative to the nanotube axis. Hysteresis loops for the pristine sample (a) and for the samples, which are irradiated with fluences of:  $10^9$  (b);  $10^{10}$  (c);  $5 \times 10^{10}$  (d);  $10^{11}$  (e);  $5 \times 10^{11} \text{ cm}^{-2}$  (f).

Table 2.

Magnetic characteristics of the samples before and after irradiation for different directions of the magnetic field relative to the nanotube axis.

Fluence $\text{cm}^{-2}$	Parallel to the nanotube		Perpendicular to the nanotube	
	$H_{C\parallel}, \text{Oe}$	$M_R/M_S$	$H_{C\perp}, \text{Oe}$	$M_R/M_S$
Pristine	48 0.10	81	0.10	
$10^9$	50	0.08	88.5	0.10
$10^{10}$	58	0.09	93	0.11
$5 \cdot 10^{10}$	48	0.08	85	0.12
$10^{11}$	46	0.08	83	0.12
$5 \cdot 10^{11}$	45	0.07	80	0.17

The different behavior of the  $M_R/M_S$  with increasing irradiation fluence for different directions of the magnetic field relative to the nanotube axis is most due not only to structural changes, but also to the nature of the defect distribution inside the nanotubes. As we showed in the works [25, 26] the moving of ions inside the nanotube facilitates the stretching of the crystallites along the nanotube with the simultaneous flow of defects to the surface of the nanotube. Two stable magnetic states are usually realized in nanotubes (magnetic moments are aligned along the axis of the nanotube or twist along the walls of the nanotube). For the samples (b)-(f) the number of defects in the direction along the axis of the nanotube decreases (by drawing the crystallites), while the number of defects at

the surface of the nanotube due to defect runoff). These structural changes will cause a decrease in the  $M_R/M_S$  for the direction of the magnetic field, parallel to the axis of the nanotubes, and increases the  $M_R/M_S$  for perpendicular applied field.

## Conclusion

Structural, morphological parameters and magnetic characteristics of Ni nanotubes with diameters of  $390 \pm 20$  nm, which were irradiated with  $\text{Fe}^{7+}$  ions with fluences up to  $5 \times 10^{11} \text{ cm}^{-2}$  and an energy of 1.5 MeV/nucleon was studied. The change in the main crystallographic characteristics after irradiation with Fe ions, are due to the appearance in the structure of defects (point defects, dislocations and the average stress), amorphous zones and formation of a new phase – FeNi. The dynamics of the main magnetic characteristics of Ni nanotubes was determined and analyzed from the position of structural changes. It was shown that change in magnetic properties is connected not only with structural changes such as defect formation, amorphization of the structure, and formation of the FeNi phase, but also with the nature of the defects distribution inside the nanotube.

## References

- [1] M. Toulemonde et al., Nuclear Instruments and Methods in Physics Research Section B: Beam Interactions with Materials and Atoms **216** (2004) 1-8.
- [2] F. Aumayr et al., Journal of Physics: Condensed Matter **23.39** (2011) 393001.
- [3] S. Rath et al., Nuclear Instruments and Methods in Physics Research Section B: Beam Interactions with Materials and Atoms **263.2** (2007) 419-423.
- [4] A.S. El-Said et al., Radiation Effects & Defects in Solids **162.7-8** (2007) 467-472.
- [5] R.P. Chauhan et.al., Journal of Radioanalytical and Nuclear Chemistry **302.2** (2014) 851-856.
- [6] R.P. Chauhan, Pallavi Rana, Radiation Measurements **83** (2015) 43-46.
- [7] A.L. Kozlovskiy et al., Vacuum **163** (2019) 103-109.
- [8] J.P. Nozieres et al., Nuclear Instruments and Methods in Physics Research Section B: Beam Interactions with Materials and Atoms **146.1-4** (1998) 250-259.
- [9] P.C. Srivastava, J.K. Tripathi, Journal of Physics D: Applied Physics **39.8** (2006) 1465.
- [10] A.S. El-Said, Nuclear Instruments and Methods in Physics Research Section B: Beam Interactions with Materials and Atoms **282** (2012) 63-67.
- [11] A. Kozlovskiy, M. Zdorovets, Materials Research Express **6.7** (2019) 075066.
- [12] A.J. Van Vuuren et al., Journal of Nuclear Materials **442.1-3** (2013) 507-511.
- [13] K.R. Nagabhushana et al., Nuclear Instruments and Methods in Physics Research Section B: Beam Interactions with Materials and Atoms **266.7** (2008) 1049-1054.
- [14] D. Gehlawat, R.P. Chauhan, Materials Chemistry and Physics **145.1-2** (2014) 60-67.

- [15] S. Panchal, R.P. Chauhan, *Physica E: Low-dimensional Systems and Nanostructures* **87** (2017) 37-43.
- [16] M. Toulemonde et al., *Nuclear Instruments and Methods in Physics Research Section B: Beam Interactions with Materials and Atoms* **216** (2004) 1-8.
- [17] A. Kozlovskiy et al., *Materials Research Express* **6.8** (2019) 085074.
- [18] H.-G. Gehrke et al., *Journal of Applied Physics* **107.9** (2010) 094305.
- [19] G. Kalkabay et al., *Journal of Magnetism and Magnetic Materials* (2019) 165436.
- [20] E.Yu. Kaniukov et al., *Materials Chemistry and Physics* **223** (2019) 88-97.
- [21] A. Kozlovskiy et al., *Ceramics International* **45.7** (2019) 8669-8676.
- [22] M.V. Zdorovets, A.L. Kozlovskiy, *Journal of Alloys and Compounds* **815** (2020) 152450.
- [23] K. Dukenbayev et al., *Nanomaterials* **9.4** (2019) 494.
- [24] A.E. Shumskaya et al., *Journal of Alloys and Compounds* **810** (2019) 151874.
- [25] A. Kozlovskiy et al., *Materials Research Express* **4.10** (2017) 105042.
- [26] M.V. Zdorovets, A.L. Kozlovskiy, *Journal of Materials Science: Materials in Electronics* **29.5** (2018) 3621-3630.